Biochemical Journal Immediate Publication. Published on 24 May 2010 as manuscript BJ20091956

Running title: Polyphosphate-containing acidic calcium stores in sea urchin eggs

Calcium and polyphosphate-containing acidic granules of sea urchin eggs are similar to acidocalcisomes but are not the targets for NAADP

Isabela B. Ramos[1,2], Kildare Miranda[2,3], Douglas A. Pace[1], Katherine C. Verbist[1], Fu-Yang Lin[4], Yonghui Zhang[5], Eric Oldfield[4,5], Ednildo A. Machado[2,3], Wanderley de Souza[2] and Roberto Docampo[1#].

[1]Department of Cellular Biology and Center for Tropical and Emerging Global Diseases, University of Georgia, Athens, GA 30602, USA, [2]Instituto de Biofísica Carlos Chagas Filho, and Instituto Nacional de Ciência e Tecnologia em Bioimagens e Biologia Estrutural, Universidade Federal do Rio de Janeiro, Rio de Janeiro, RJ 21941, Brazil, [3]Instituto Nacional de Metrologia Normalização e Qualidade Industrial, Diretoria de Programas, Xerém, Rio de Janeiro, RJ 25250, [4]Center for Biophysics and Computational Biology and [5]Department of Chemistry, University of Illinois at Urbana-Champaign, Urbana, IL 61801

[#]To whom correspondence should be addressed at: Department of Cellular Biology, and Center for Tropical and Emerging Global Diseases, University of Georgia, 350B Paul D. Coverdell Center, 500 D.W. Brooks Dr., Athens, GA 30602, Tel: 706-542-8104; Fax: 706-542-9493; Email: rdocampo@uga.edu

The abbreviations used are: ASW, artificial sea water; cADP ribose, cyclic adenosine diphosphate ribose; DAPI, 4',6'-diamidino-2-phenylindole; GluIM, gluconate intracellular-like medium; GPN, glycyl-L-phenylalanine-naphthylamide; IP_3, inositol 1,4,5-trisphosphate, NAADP, nicotinic adenine dinucleotide phosphate; P_i, phosphate; PP_i, pyrophosphate; poly P, polyphosphate; PPase, pyrophosphatase; PPBD, poly P binding domain of exopolyphosphatase; PPX, exopolyphosphatase; RFU, relative fluorescence units.

Synopsis

Acidocalcisomes are acidic calcium storage compartments described from bacteria to man and characterized by their high content in polyphosphate (poly P), a linear polymer of many tens to hundreds of orthophosphate residues linked by high energy phosphoanhydride bonds. Here we report that millimolar levels of short-chain poly P (in terms of P_i residues) and inorganic pyrophosphate are present in sea urchin extracts as detected using ^{31}P NMR, enzymatic determinations, and agarose gel electrophoresis. Poly P was localized to granules randomly distributed in the sea urchin eggs as shown by labeling with the poly P binding domain of *Escherichia coli* exopolyphosphatase. These granules were enriched using iodixanol centrifugation and shown to be acidic and to contain poly P, as determined by acridine orange and 4',6'-diamidino-2-phenylindole (DAPI) staining, respectively. These granules also contained large amounts of calcium, sodium, magnesium, potassium and zinc, as detected by X-ray microanalysis, and bafilomycin A_1-sensitive ATPase, pyrophosphatase and exopolyphosphatase activities, as well as Ca^{2+}/H^+ and Na^+/H^+ exchange activities, being therefore similar to acidocalcisomes described in other organisms. Calcium release from these granules induced by

nigericin was associated with poly P hydrolysis. Although NAADP released calcium from the granule fraction, this activity was not significantly enriched as compared with the NAADP-stimulated calcium release from homogenates and was not accompanied by polyphosphate hydrolysis. Glycyl-L-phenylalanine-naphthylamide (GPN) released calcium when added to sea urchin homogenates, but was unable to release calcium from acidocalcisome-enriched fractions, suggesting that these acidic stores are not the targets for NAADP.

Key words: acidocalcisome, calcium, GPN, polyphosphate, sea urchin eggs, vacuolar H^+-ATPase

INTRODUCTION

The sea urchin egg has been an invaluable model for studying Ca^{2+} homeostasis and signaling. Intracellular Ca^{2+} increases upon fertilization and is important for the generation of the fertilization envelope and for initiation of the biochemical events that serve to wake the egg from a state of dormancy [1].

A number of second messengers able to release Ca^{2+} from different intracellular stores were described for the first time in sea urchin eggs, such as cyclic adenosine diphosphate ribose (cADPR) [2] and nicotinic acid adenine dinucleotide phosphate (NAADP) [3]. While cADPR and inositol 1,4,5-trisphosphate (IP_3), release Ca^{2+} from the endoplasmic reticulum of sea urchin eggs, NAADP does it from acidic vesicles that were proposed to be lysosome-like organelles [4], possibly the so-called yolk platelets [5]. NAADP was also shown to increase the pH of these acidic vesicles by a mechanism coupled to Ca^{2+} release via the NAADP receptor [6]. It was proposed that the fall in the luminal [Ca^{2+}] allows H^+ to bind to vacated sites on a luminal polyanionic matrix thus resulting in alkalinization of the store [6].

The findings that NAADP released Ca^{2+} from acidic organelles of sea urchin eggs [4] led to investigations as to whether NAADP was also able to mobilize Ca^{2+} from lysosomes of mammalian cells. NAADP was shown initially to release Ca^{2+} from acidic organelles of pancreatic acinar and β-cells [7, 8], coronary artery myocytes [9], and pheochromocytoma cell line PC12 [10], but apparently not from T lymphocyte cell lines [11, 12]. It was found that NAADP-induced Ca^{2+} release was associated with endolysosomal function because the Ca^{2+} release response was dependent on a proton gradient maintained by an ATP-dependent vacuolar-type proton pump that is primarily present in the endocytic pathway [13]. Accumulating evidence showed that this NAADP-sensitive Ca^{2+} store was unique and distinct from IP_3- and cADPR-sensitive Ca^{2+} stores [14, 15], and results suggested that, at least in rat liver, it is the lysosome [13]. Two-pore channels have recently emerged as potential receptors for NAADP in the lysosomes of mammalian cells [16-18], and they have now been identified as NAADP targets for Ca^{2+} release in the sea urchin [19].

Sea urchin eggs have a number of intracellular vesicles and several types of granules in their cytoplasm, as identified by electron microscopy. Among them the cortical granules, which are located close to the surface and are exocytosed upon fertilization and formation of the fertilization envelope, the yolk platelets, which are an abundant group of organelles of high and uniform electron-density and that can occupy approximately half the volume of the egg [20], and the clear granules [21, 22] characterized by their clear appearance, that are distributed at random in the unfertilized eggs [21]. Both the cortical granules [4] and the clear granules [21] are acidic,

while the yolk platelets increase their acidity from pH 6.8 to pH 6.1 upon fertilization [23]. These changes in pH in yolk platelets (alkalinization on NAADP stimulation and acidification upon fertilization) reveals the multiphasic nature of this phenomenon with NAADP-induced response being a "rapid" response whereas acidification upon fertilization being a "slow" response.

Yolk platelets have been proposed to be the acidic organelles responsible for Ca^{2+} release upon NAADP stimulation [4, 5]. This is in agreement with experiments using eggs stratified by centrifugation. Under these conditions yolk platelets localize to the centrifugal pole, which is the site where the higher Ca^{2+} release occurs upon local photolysis of caged NAADP [24] and is opposite to the nucleus and lipid droplets. However, photolysis of NAADP at the centripetal pole, which is the region where clear granules localize, also results in a transient Ca^{2+} release [24]. Interestingly this region of clear granules is the one more intensely labeled with acridine orange [21], suggesting that clear granules are more acidic than yolk platelets. In contrast LysoTracker Red appears to label preferentially the yolk platelets [4] and this labeling disappears after treatment with glycyl-L-phenylalanine-naphtylamide (GPN), a substrate of the lysosomal cathepsin C that selectively disrupts these organelles via osmotic lysis [25]. Interestingly, although yolk platelets are distributed at random in the sea urchin egg, NAADP induces a peripheral vesicular alkalinization even when injected in the middle of the egg suggesting the presence of a subpopulation of NAADP-sensitive stores [6].

The clear granules of sea urchin eggs are morphologically very similar to acidocalcisomes, which are lysosome-related organelles characterized by their abundant content of the polyanion polyphosphate (poly P) bound to cations such as calcium, magnesium, and zinc [26]. Acidocalcisomes are present in trypanosomatid and apicomplexan parasites [26], as well as in the green algae *Chlamydomonas reinhardtii* [27], and the slime mold *Dictyostelium discoideum* [28], and were also identified in bacteria [29, 30], human platelets [31], and insect [32] and chicken [33] eggs. As acidocalcisomes are acidic, rich in Ca^{2+} and in the polyanion poly P, and it has been shown that Ca^{2+} can be released from them after their alkalinization with NH_4Cl or by the K^+/H^+ ionophore nigericin [34], we investigated whether some of the acidic granules of sea urchin eggs are equivalent to acidocalcisomes, and whether they are also targets for NAADP-stimulated Ca^{2+} release.

MATERIALS AND METHODS

Chemicals and reagents

ATP, nigericin, valinomycin, 4' 6-diamidino-2-phenylindole (DAPI), inositol 1,4,5-trisphosphate; nicotinic acid adenine dinucleotide phosphate, pyrophosphate, tripolyphosphate (poly P_3), poly P_{75+}, and protease inhibitors (P8340) were purchased from Sigma Chemical Co. Coomassie Blue protein assay reagent was from Bio-Rad. The anti-Xpress epitope monoclonal antibody and Fluo-3 were from Invitrogen. Bafilomycin A_1 was from Kamiya Biomedical, Thousand Oaks, CA. *Escherichia coli* strain CA38 pTrcPPX1 was kindly provided by Prof. Arthur Kornberg (Stanford University School of Medicine, Stanford, CA). *E. coli* DH5α harboring pTrc-PPBD was provided by Dr. Katsuharu Saito (Shinshu University, Nagano-Ken, Japan). LysoTracker Red DND-99 was from Invitrogen. All other reagents were of analytical grade.

Egg collection and homogenate preparation

Sea urchins were obtained from Gulf Specimen Marine Lab (Panacea, FL) or from the Guanabara Bay (Rio de Janeiro, Brazil). Eggs from *Lytechinus variegatus* or *Arbacia punctulata* were harvested by intracoelomic injection of 0.5 M KCl and collected in artificial sea water (ASW: 435 mM NaCl; 40 mM $MgCl_2$; 15 mM $MgSO_4$; 11 mM $CaCl_2$; 10 mM KCl; 2.5 mM $NaHCO_3$ and 20 mM Tris base, pH 8.0). Egg homogenates were prepared as described elsewhere [6]. Briefly, eggs were washed four times in Ca^{2+}-free ASW (the first two washes containing 1 mM EGTA) and then washed in gluconate intracellular-like medium without ATP-generating system (GluIM: 250 mM potassium gluconate, 250 mM *N*-methylglucamine, 20 mM Hepes, and 1 mM $MgCl_2$, pH 7.2). Eggs were then homogenized in the same medium in the presence of protease inhibitors (P8340, Sigma). The homogenate (50%, v/v) was centrifuged at 13000 ***g*** for 10 sec at 4°C, and the supernatant was sequentially diluted in equal volumes of GluIM over a period of 3 h, as described before [6]. Microscopy experiments were done with both species of sea urchin eggs with similar results. All other experiments were done using *Lytechinus variegatus* eggs.

Isolation of dense granules

The egg homogenate (8 ml, ~ 4 x 10^5 eggs/ ml) was centrifuged at 5000 ***g*** for 10 min at 4°C. The supernatant (4 ml) was then loaded to the top of a 20% iodixanol fractionation medium (OptiPrep™, Greiner Bio-One) diluted in GluIM buffer (20 ml). The preparation was centrifuged at 60,000 ***g*** for 60 min at 4°C. The pellet was resuspended in 100 µl GluIM buffer, washed at least 3 times in GluIM, and used as dense granule fraction.

Electron microscopy and X-ray microanalysis

For imaging whole cells and dense granule fractions, they were washed first in 100 mM Hepes buffer, pH 7.4, and directly applied to Formvar-coated 200-mesh copper grids, allowed to adhere for 10 min at room temperature, blotted dry, and observed directly in an energy-filtering Zeiss 902 transmission electron microscope. This treatment avoided salt precipitation. Electron energy-filtered images were taken at an energy loss of 70 eV using a spectrometer slit width of 10 eV. For X-ray microanalysis, samples were examined in a JEOL 1200 EX transmission electron microscope. X-rays were collected for 150 s using a Si (Li) detector with Norvar window on a 0 to 10 KeV energy range with a resolution of 10 eV/channel. Analysis was performed using a Noran Voyager III analyzer with a standard analysis identification program. No changes in the size of the organelles were detected when the fractions were suspended in 100 mM Hepes, pH 7.4, plus 300 or 400 mM sucrose, instead of 100 mM Hepes alone.

For conventional electron microscopy eggs and dense granule fractions were fixed in 4% formaldehyde, 2.5% glutaraldehyde diluted in 0.1 M sodium cacodylate buffer (pH 7.3) at 4°C for 24 h, and then embedded in epoxy resin, sectioned and stained using standard methods. To verify that osmotic conditions did not change the size of organelles, the fixative was also diluted in ASW but no changes in the morphology of different organelles were observed.

Extraction of PP_i and long- and short-chain polyphosphate (poly P)

Egg homogenates were centrifuged at 16000 ***g*** for 30 min at 4°C and the pellet was treated with methods to extract either long-chain or short-chain poly P and PP_i. Different samples were used for each method. Aliquots of known volumes from different steps of the dense granule fraction separation were also obtained and centrifuged at 14000 ***g*** for 30 min at 4°C. The pellets were extracted and used for poly P and PP_i determinations. Long-chain (LC) poly P extraction was performed as described by Ault-Riché et al. [35]. Short-chain (SC) poly P and PP_i extraction was done as described by Ruiz et al., [34]. For NMR, EDTA was added to the extracts to a final concentration of 25 mM prior to adjusting to pH 7.0. All the extracts contained 10% D_2O (v/v) to provide a field-frequency lock. Protein measurements were performed using the Bradford protein assay kit (Bio-Rad).

Analysis of PP_i and poly P

Poly P levels were determined from the amount of phosphate (P_i) released upon treatment with an excess of recombinant *Saccharomyces cerevisiae* exopolyphosphatase 1 (rPPX1). The recombinant enzyme was prepared as described before [34]. Aliquots of long- and short-chain poly P extracts (always less than 1.5 nmol) were incubated for 15 min at 37°C with 60 mM Tris-HCl, pH 7.5, 6.0 mM $MgCl_2$, and 3000-5000 units of purified rPPX1 in a final volume of 100 µl. One unit corresponds to the release of 1 pmol of P_i/min at 35°C. Release of P_i was monitored by the method of Lanzetta et al. [36]. For PP_i quantification, the procedure was essentially the same, but using an excess of soluble thermostable inorganic pyrophosphatase (TiPPase, New England Biolabs), 0.04 U per reaction, in 50 mM Tris, pH 7.5, 5 mM $MgCl_2$, for 30 min at 35°C. To detect poly P degradation by dense granule fractions in the presence of 10 µM nigericin, aliquots were collected after 5, 10 and 15 min, centrifuged at 14000 ***g*** for 10 sec and the pellets used for poly P extraction and determinations, as described above. The intracellular concentration of phosphate compounds was calculated taking into account a volume of 904 pl/ egg.

NMR spectroscopy

For NMR analyses, EDTA was added to poly P extracts to a final concentration of 25 mM prior to adjusting to pH 7.0. All the extracts contained 10% D_2O (v/v) to provide a field-frequency lock. Phosphorus NMR spectra were acquired at 242.8 MHz using a Varian INOVA NMR spectrometer equipped with a 14.1-Tesla Oxford Instruments magnet. For perchloric acid extracts, 10,784 transients were collected at room temperature using 25 µs (90°) pulse excitation, a 20-kHz spectral width, 32,768 data points, and a 5-s recycle time. Inverse gated proton decoupling was used to remove NOE and J-coupling effects. The chemical shifts of all the ^{31}P spectra were referenced to 0 ppm using an 85% phosphoric acid external standard. The specific assignments of individual resonances were based on published chemical shifts and ^{31}P-^{31}P scalar couplings, and in some cases, co-addition of authentic compounds. NMR spectra were processed using the MacNuts 0.9.4 program (Acorn NMR, Inc.) and included base-line correction, zero-filling, and a 2-Hz exponential line broadening prior to Fourier transformation.

Fluorescence microscopy

For poly P localization in whole eggs the recombinant poly P binding domain (PPBD) of *Escherichia coli* exopolyphosphatase linked to an Xpress epitope tag was used, as previously

described [37]. Briefly, eggs suspended in ASW were permeabilized with 0.1% Triton X-100 for 2 min. After washing in Tris buffered saline pH 7.2 (TBS) (100 mM Tris-HCl, pH 7.2, 150 mM NaCl), eggs were incubated in blocking buffer (3% BSA in TBS, pH 7.2) for 30 min. Eight µg/ml of PPBD and 10 µg/ml of anti-Xpress epitope monoclonal antibody were added and the samples incubated for 1 h under gentle agitation. The samples were washed with blocking buffer and TBS and fixed in 4% paraformaldehyde diluted in TBS for 30 min. After fixation the eggs were blocked for 15 min in 100 mM NH_4Cl in TBS, and for additional 30 min in blocking buffer plus 0.1% Tween 20. Secondary antibodies (Alexa Fluor^{tm} 488 goat anti mouse IgG, Invitrogen) were diluted in the same buffer (1:1000) and incubated with the eggs for 1 h under gentle agitation. After washing in blocking buffer plus Tween 20, the samples were observed using an Olympus IX-71 fluorescence microscope with a Photometrix CoolSnap$_{HQ}$ CCD (charge-coupled device) camera driven by Delta Vision software (Applied Precision) using filters with excitation at 480-500 nm and emission at 510-550 nm. For the egg 3-D projection (supplemental movie 1), z-stacks were acquired and reconstructed using the same software described above.

For localization of acridine orange and DAPI, the dense granule fraction was incubated with 3 µM acridine orange or 10 µg/ml DAPI for 10 min at room temperature in the presence of protease inhibitors cocktail (Sigma, P8340), 2 µg/ml oligomycin and 2 µg/ ml antimycin, and observed in the microscope described above with excitation at 340-380 nm for DAPI and at 450-490 nm for acridine orange, and emission >500 nm for both dyes.

Egg stratification

Egg stratification was done as reported previously [4, 24]. PPBD and DAPI staining were performed as described above. For Lysotracker staining eggs were incubated with 0.5 nM LysoTracker Red DND-99 for 30 min at room temperature before stratification [4] and then stained with PPBD as described above.

Fluorometry

H^+ movements, and Ca^{2+} release were monitored using a fluorometer (F4500, Hitachi Instruments). H^+ movements were monitored by following changes in acridine orange (6 µM) fluorescence (excitation at 495 nm, emission at 530 nm) after incubating dense granule fractions (50-80 µg protein for bafilomycin experiments; 600-800 µg of protein for Na^+/H^+ and Ca^{2+}/H^+ experiments) in 2 ml of GluIM containing 2 µg/ml oligomycin, and 2 µg/ml antimycin A. Acridine orange was allowed to equilibrate for 2-5 min, while the dye partitioned into dense granules, and then valinomycin (10 µM), bafilomycin A_1 (1 µM), and/or nigericin (5 µM) were added as indicated. Ca^{2+} release was measured following changes in the fluorescence (excitation 506 nm, emission 526 nm) of Fluo-3 (3 µM). Total homogenates and dense granule fractions (310 µg of protein for NAADP experiments; 600-800 µg of protein for GPN experiments) were diluted in 2 ml of GluIM buffer. IP_3 (300 nM), NAADP (200 nM) and nigericin (5 µM) were added where indicated in the figures.

Gel electrophoresis

Perchloric acid extracts were dried in a speed vac and resuspended in 60 mM Tris-HCl, pH 7.5, 6.0 mM $MgCl_2$. For PPX treated samples rPPX1 [34] was added (3000-5000 units) in a final volume of 50 µl and incubated for 30 min at 35°C. Poly P samples were then mixed with DNA loading buffer (10 mM Tris-HCl, pH 7.5, 10 mM EDTA, 0.25 % Orange-G and 0.65 % sucrose) and loaded into 1-2% agarose gels. The gels were run at 200 V in Tris-acetate pH, 8.2, 1 mM EDTA (TAE buffer) until the dye (Orange-G) reached the middle of the gel. The gels were then stained with 0.1 % toluidine blue for 1 h and then de-stained with several changes of deionized water for 4 h.

PPX and PPase activities in the dense granule fraction

Dense granule fractions were homogenized using a Teflon pestle tissue homogenizer in ice-cold reaction buffer for exopolyphosphatase (PPX) (20 mM Tris, 5 mM magnesium acetate, 100 mM ammonium acetate, pH 7.5), or pyrophosphatase (PPase) (50 mM Tris, 5 mM $MgCl_2$, pH 7.5) activities, and supplemented with protease inhibitors cocktail (Sigma P8340). To these samples, 0.1 mM poly P_{75+} or 0.1 µM PP_i were added and aliquots were collected at 5, 10 and 15 min after substrate addition. The aliquots were centrifuged 14000 ***g*** for 10 sec and the pellets were processed for poly P and PP_i determinations as described before. Controls were performed with no sample, incubating the substrates in plain buffer under the same conditions.

Data analysis

All results are expressed as means ± S.D., or, when appropriate, standard error of the mean (S.E.M.) for n different experiments. Statistical significance was determined by Student's t test or by one way ANOVA at $P < 0.05$.

RESULTS

Ultrastructure and elemental analysis of sea urchin egg granules

Ultrastructural analysis of sea urchin eggs allowed the identification of several granules. The cortical granules (whose size varies from 0.39 ± 0.02 to 0.92 ± 0.05 µm diameter in different sea urchin species [38]) are located close to the surface and are identified by the presence of star-like dense material in their interior (cg, Figs. 1A, *thin arrow*). An abundant group of organelles of about 1 to 2 µm diameter, oval form, and high and uniform electron-density are known as yolk platelets (YP, Fig. 1A-E) [20]. In addition, clear granules [21, 22], characterized by their clear appearance and the presence in most of them of an electron-dense material in various states of condensation (Fig. 1A-E, *thick arrows*), are distributed at random in the unfertilized eggs [20]. These clear granules, of average diameter of 0.83 ± 0.29 µm, are very similar in their appearance to the acidocalcisomes described in different organisms [26]. A large number of other clear granules that are smaller (average diameter 0.19 ± 0.04 µm) than the granules described above but which also have similar appearance to acidocalcisomes (empty appearance with a thin layer of dense material that sticks to the inner face of the membrane; Figs. 1B and 1E, *white arrowheads*), and mitochondria (Figs. 1B and 1D, *black arrowheads*) are also visible.

To investigate whether the clear granules correspond to acidocalcisomes, whole cell mounts of sea urchin eggs or homogenates were analyzed by energy-filtering transmission electron

microscopy. Using this technique the contrast of a given structure in the image solely arises from its mass density since these preparations are not stained. Many electron-dense vesicles of varying diameter (average 0.73 ± 0.09 μ m) were seen in intact eggs (Fig. 2A, *black arrows*) or homogenates (Fig. 2B, *black arrow*). Other larger and less electron-dense vesicles (probably yolk platelets) were also observed (Fig. 2B, *white arrow*). X-ray microanalysis of these vesicles was performed (Figs. 2C, and 2D). All ten spectra of the very electron-dense vesicles taken from different homogenates were qualitative similar showing considerable amounts of oxygen, sodium, magnesium, phosphorus, sulfur, calcium, and zinc concentrated in their matrix (Fig. 2C). X-ray microanalysis of the less electron dense granules, probably corresponding to yolk platelets (Fig. 2B, *white arrow*), revealed only the presence of sulfur (Fig. 2D), suggesting that they are rich in proteins. Copper arose from the Formvar-coated grids in both cases and was also detected in spectra taken from the background (not shown).

PP_i and poly P in sea urchin eggs

One of the characteristics of acidocalcisomes is that they contain large amounts of short- and long-chain poly P and also PP_i [26]. As shown in Fig. 3A egg homogenates contain ~220-fold more short-chain than long-chain poly P while PP_i content was about half the amount of short-chain poly P (all expressed in terms of P_i residues for comparative purposes). Poly P was also detected by electrophoresis of extracts in 1% agarose gels stained with toluidine blue (Fig. 3B, *lane 1*), and pretreatment of these samples with exopolyphosphatase (rPPX1) resulted in considerable decrease in staining (Fig. 3B, *lane 2*).

Fig. 3C shows a representative 242.8 MHz (^{1}H-decoupled) ^{31}P NMR spectrum of perchloric acid extracts of sea urchin eggs. Resonance assignments for this spectrum are given in Table 1. The predominant peak in the spectrum is inorganic phosphate (peak B). The inset region at ~-6 ppm (*left inset*) contains the pyrophosphate resonance, peak F. The region between -19 and -22 ppm is shown in the *right inset* and contains peaks for the β phosphate of nucleoside triphosphates (M), in addition to the central phosphate of poly P (L). The spectrum shows considerable amounts of phosphorylcholine (A) and phosphoarginine (C).

Poly P, as detected using the poly P binding domain (PPBD) of *S. cerevisiae* exopolyphosphatase (PPX) [37], was localized in small vesicles randomly distributed in the egg (Fig. 3D and 3E, and supplementary movie 1). There was no poly P signal in the negative controls (i.e. in the absence of PPBD).

Isolation of dense granules and demonstration of their acidity and poly P content

To isolate the dense granules (Fig. 2) and investigate their chemical and enzymatic content, we used iodixanol centrifugation as described under Material and Methods. The pellet fraction was applied to Formvar-coated grids, and direct observation evidenced the presence of multiple electron dense granules of variable size (Supplementary Fig. 1A). X-ray microanalysis (Supplementary Fig. 1B and 1C) showed that most of these granules (15/25) contained similar elemental composition to that of dense granules in whole eggs or homogenates (Fig. 2C). Standard transmission electron microscopy of this fraction revealed the presence of clear granules (corresponding to dense granules), which most of the times appeared empty or containing a residual electron dense material, as previously observed in whole eggs (Fig. 1), and some mitochondrial contamination (data not shown).

The presence of granules in the dense fraction was confirmed by incubation of the preparation in the presence of acridine orange. The acridine orange-stained granules appeared in groups (Fig. 4A) or as isolated vesicles (Fig. 4C). We also investigated the location of poly P using DAPI (Fig. 4B and 4D). DAPI is known to shift its emission fluorescence to a maximum wavelength of 525 nm (yellow) in the presence of poly P, this change being specific for poly P and not produced by PP_i or other anions [31]. We detected the staining of numerous vesicles, either in groups (Fig. 4B) or isolated (Fig. 4D). No staining was detected when DAPI was omitted (data not shown).

Work by Morgan and Galione [6] has shown that acidification of granules in sea urchin eggs is maintained by a vacuolar type H^{+-}ATPase (V-H^+-ATPase), as it happens with other acidic organelles, including the acidocalcisomes of *T. cruzi* [39], *T. brucei* [40], *D. discoideum* [28], *C. reinhardtii* [27], and human platelets [31]. Interestingly, the function of this proton pump could be demonstrated only by inhibition of acidification by bafilomycin A_1 after preincubation of the preparation with either valinomycin or FCCP [6]. In agreement with those results, bafilomycin A_1 released acridine orange after preincubation of the dense granule fractions with valinomycin (Fig. 4E, *black trace*) but not in its absence (Fig. 4E, *grey trace*), although this could be accomplished by nigericin (Fig. 4E, *grey trace*). Addition of nigericin after bafilomycin A_1 completed the release of acridine orange from the vesicles (Fig. 4E, *black trace*).

Evidence for Na^+/H^+ and Ca^{2+}/H^+ exchange activities in dense granules

Acidocalcisomes of *Trypanosoma brucei* [40, 41] and *Leishmania donovani* [42, 43] have been reported to contain Na^+/H^+ and Ca^{2+}/H^+ exchangers and the coupled interaction of these exchangers was postulated to result in a mechanism of Ca^{2+} release upon alkalinization or Na^+ entry into acidocalcisomes [42]. Experiments on enriched dense granule fractions showed the presence of these ion exchange mechanisms. For example, addition of 100 mM NaCl (Fig. 4F, *black trace*) but not of 100 mM KCl (Fig. 4F, *light gray trace*) resulted in acridine orange efflux, suggesting the activity of a Na^+/H^+ exchanger in the dense granule fraction. Addition of 10 and 50 µM $CaCl_2$ under similar conditions also resulted in acridine orange efflux (Fig. 4G, *black* and *dark gray traces*, respectively), suggesting the operation of a Ca^{2+}/H^+ exchanger, and the potential function of these exchangers as a mechanism of Ca^{2+} release upon alkalinization of dense granules [43]. Under physiological conditions these exchangers could contribute to Na^+ and Ca^{2+} uptake into these acidic compartments, as occurs with the plant vacuole [44].

Association of Ca^{2+} release and poly P hydrolysis

It has been shown that Ca^{2+} release from acidocalcisomes of *T. cruzi* occurs in parallel with poly P hydrolysis [34]. We therefore investigated whether there was a correlation between Ca^{2+} release from the acidic compartment containing poly P in the sea urchin egg dense granule fraction, and poly P hydrolysis. Addition of nigericin resulted in Ca^{2+} release from the dense granule fraction, as detected by changes in the fluorescence of Fluo-3 (Fig. 5A) and this resulted in a significant decrease in the levels of short-chain poly P but not in the levels of long-chain poly P (Fig. 5C). Addition of nigericin also resulted in alkalinization of the vesicles (Fig. 5B) confirming the link between alkalinization of acidocalcisomes and Ca^{2+} release.

Degradation of Poly P and PP_i in dense granules

Acidocalcisomes are known to possess enzymes linked to PP_i and poly P metabolism [26]. The rapid hydrolysis of poly P that occurs when Ca^{2+} release is stimulated by nigericin (Fig. 5) suggested the presence of an exopolyphosphatase activity in the dense granule fraction. To know whether this was the case, we investigated PP_i and poly P hydrolysis by dense granule fractions. Hydrolysis of poly P_3 (Fig. 6A) or PP_i (Fig. 6B) was approximately linear with time while hydrolysis of poly P_{75+} stopped after 5 min. This probably indicates the hydrolysis of contaminating short-chain poly Ps in the poly P_{75+} sample (which is a mixture of poly Ps of mean length of 84), and the inability of the polyphosphatase to cleave long-chain poly Ps.

NAADP-stimulated Ca^{2+} release from dense granules is not accompanied by hydrolysis of poly P and the fraction is not sensitive to GPN

NAADP has been shown to release Ca^{2+} from acidic granules of sea urchin eggs [4], while IP_3 releases Ca^{2+} from the endoplasmic reticulum [2]. Figs. 7A and 7D show that both NAADP and IP_3 were able to release comparable amounts of Ca^{2+} from vesicular compartments in egg homogenates. A second addition of NAADP showed no response revealing desensitization (data not shown). NAADP was, however, less efficacious in the dense granule fraction (Fig. 7B) or IP_3 (Fig. 7E). We tested whether poly P hydrolysis occurred as a consequence of Ca^{2+} release by NAADP in dense granule fractions but no significant changes were detected (Fig. 7G). The lack of enrichment in NAADP-sensitive calcium stores, together with the lack of poly P hydrolysis accompanying calcium release by NAADP suggest that the acidocalcisome-related organelles of sea urchin eggs are not the calcium stores sensitive to NAADP.

The presence of releasable Ca^{2+} in lysosomes has been demonstrated based on experiments using glycyl-L-phenylalanine-naphthylamide (GPN) and it has been reported that NAADP-targeted stores are sensitive to GPN [4]. GPN is a lysosome-disrupting cathepsin-C substrate that was originally used to distinguish lysosomes, which contain cathepsin C, from prelysosomal endocytic vacuoles, which do not [25]. Hydrolysis of GPN by cathepsin C induces osmotic swelling of the lysosome and release of its content, including Ca^{2+}, into the cytoplasm. Treatment of sea urchin homogenates with GPN caused Ca^{2+} release, which was completed by nigericin (Fig. 7H, *trace 2*). In contrast, addition of GPN to dense granule fractions did not cause Ca^{2+} release (Fig. 7H, *trace 1*) suggesting that this fraction is not contaminated with lysosomes.

Use of stratified eggs reveals that dense granules localize to the centripetal pole of the egg

As discussed above when eggs are stratified by centrifugation yolk platelets localize to the centrifugal pole which is the site where higher Ca^{2+} release occurs upon local photolysis of caged NAADP and which is opposite to the nucleus and lipid droplets, where clear granules localize [24]. When eggs were stratified and stained with either PPBD (supplementary Figs. S2B, and 2C) or DAPI (supplementary Figs. S2E, and 2F), staining was detected in the centripetal pole in agreement with the reported localization of the clear granules [24] and with the results showing negligible NAADP-stimulated Ca^{2+} release by dense granule fractions. In contrast, staining with LysoTracker Red was in the centrifugal pole, where the yolk platelets localize and where higher NAADP-stimulated Ca^{2+} release has been detected [4] (Figs. 2G-J).

DISCUSSION

We report here that sea urchin eggs are rich in poly P. Poly P was detected by a biochemical method based on its specific hydrolysis by an exopolyphosphatase, by toluidine blue staining in agarose gels, by ^{31}P NMR, and by a recently developed method based on staining with the specific poly P binding region of *S. cerevisiae* PPX [37]. This was confirmed by visualization of poly P in the dense granule fraction using DAPI and by its hydrolysis when nigericin released Ca^{2+} from these fractions. We also found considerable amounts of phosphoarginine, a phosphagen present in many invertebrates although not previously reported in sea urchin eggs [45].

Our results also suggest that the dense granules of sea urchin eggs, which could correspond to the clear granules detected by transmission electron microscopy (both large and small, Fig. 1) have many characteristics in common with acidocalcisomes [26]: 1) they are acidic due to the operation of a bafilomycin A_1-sensitive vacuolar ATPase and are able to accumulate acidophilic dyes such as acridine orange; 2) they can store extremely large amounts of calcium and other cations such as magnesium, sodium and zinc, and can release Ca^{2+} in the presence of nigericin; 3) they contain very large amounts of phosphorus in the form of phosphate, pyrophosphate, and poly P; 4) they have very high electron density, when examined by energy-filtering transmission electron microscopy, and have an empty appearance with condensed material in their interior, when examined by standard transmission electron microscopy; and 5) they possess activities commonly found in acidocalcisomes, such as pyrophosphatase [46], exopolyphosphatase [47], and Ca^{2+}/H^+ and Na^+/H^+ exchangers [40-43].

Clear granules are distributed at random in unfertilized sea urchin eggs [21], in agreement with the distribution of poly P-labeled granules (Fig. 3E, and supplementary movie 1). The function of these clear granules is unknown, but their composition, investigated in this work, implies an important role in storage of phosphorus and cations needed for embryo development. Our results suggest that although these granules are acidic and contain large amounts of calcium they are not the targets for NAADP-stimulated Ca^{2+} release.

It has been reported that fertilization induces pH changes in acidic stores of sea urchin eggs [5], and we have demonstrated that alkalinization of dense granules leads to Ca^{2+} release and poly P hydrolysis. Alkalinization of acidic stores of the sea urchin egg could be either upon vesicle fusion with the plasma membrane, when the alkaline extracellular medium exchanges with the acidic lumen of cortical granules that are the primary egg exocytic vesicles, or upon Ca^{2+} release from yolk platelets stimulated by NAADP [5]. It has been reported that cortical alkalinization coincides with NAADP-induced Ca^{2+} release from intracellular stores [5], and that this alkalinization appears to occur at the individual vesicle level [5]. Alkalinization of yolk platelets is increased by NAADP by a mechanism coupled to Ca^{2+} release via the NAADP receptor [5]. It has been proposed that the fall in the luminal [Ca^{2+}] allows H^+ to bind to vacated sites on a luminal polyanionic matrix thus resulting in alkalinization of the store [6].

In addition to acidic store alkalinization, it has been shown that fertilization of sea urchin eggs led to a change in cytosolic pH from 6.9 to 7.3 with a concomitant acidification of the sea water, and that the egg remains alkaline for approximately 60 min [48, 49]. This change in cytosolic pH is driven by a plasma membrane sodium-proton exchanger [48]. An increase in cytosolic sodium has been shown before to increase the release of calcium from acidocalcisomes of *Trypanosoma brucei* [40, 41] and *Leishmania donovani* [42, 43] and this could potentially occur with the sea urchin egg dense granules. It has also been shown that suspension of sea

urchin eggs in NH_4Cl (5 mM, pH 8.0), which could lead to alkalinization of all acidic granules, stimulates their metabolism and ability to undergo chromosome replication and condensation without triggering the cortical granule reaction [50]. Therefore, we cannot rule out that alkalinization of dense granules could lead to an additional Ca^{2+} release.

Previous studies have indicated that the acidic compartments responsible for Ca^{2+} release induced by NAADP are lysosome-like organelles [4], possibly the yolk platelets [5]. This was based on experiments showing that GPN-mediated disruption of the organelles reduced the response to photoreleased or microinjected free NAADP, and on the response of yolk platelets-enriched fractions to NAADP [4]. The lack of calcium detection in yolk platelets in our X-ray microanalyses (Fig. 2D) does not indicate its absence but simply that the amount of calcium present is below the limit of detection of this technique, which cannot discriminate between bound and free calcium. Yolk platelets would then be equivalent to the lysosomes of mammalian cells that are emerging as important calcium stores [51], while the clear (dense) granules would be, as acidocalcisomes, equivalent to lysosome-related organelles [51].

NAADP-induced Ca^{2+} signals are small and possibly localized but can trigger endoplasmic reticulum Ca^{2+} mobilization through Ca^{2+}-induced Ca^{2+} release via IP_3 and ryanodine receptors [17], thus explaining the extensive Ca^{2+} waves detected after fertilization. Alkalinization of the cytosol and Ca^{2+} release from dense granules (acidocalcisomes) could also contribute to these Ca^{2+} waves. Supplementary Fig. 3 shows a model of the Ca^{2+} mobilization pathways that could be involved in sea urchin eggs. NAADP would trigger Ca^{2+} release from yolk platelets that could then trigger endoplasmic reticulum Ca^{2+} mobilization through Ca^{2+}-induced Ca^{2+} release via IP_3 and ryanodine receptors. Alkalinization of the egg cytoplasm by Na^+ entry would release additional Ca^{2+} from dense granules (acidocalcisomes). Therefore acidocalcisomes, which are randomly distributed, could contribute to the NAADP-mediated two phase Ca^{2+} release response. Alkalinization of these acidocalcisomes would lead to the hydrolysis of poly P, which would provide an important source of P_i for the anabolic reactions necessary for embryogenesis.

We thank the late Prof. Arthur Kornberg for *E. coli* CA38 pTrcPPX1, and Dr. Katsuharu Saito for *E. coli* DH5a pTrc-PPBD. This work was supported by the Georgia Research Alliance/Barbara and Sanford Orkin Chair in Tropical and Emerging Global Diseases and Cellular Biology (to R.D.). I.B.R. was supported in part by a training grant from the Ellison Medical Foundation to the Center for Tropical and Emerging Global Diseases. E.O., F.-Y.L and Y.Z. were supported in part by NIH grant GM65307. I.B.R., K.M., E.A.M., and W.S. were supported in part by the Fundação de Amparo a Pesquisa do Estado de Rio de Janeiro (FAPERJ) and the Conselho Nacional de Desenvolvimento Tecnológico (CNPq, Brazil).

REFERENCES

1. Parrington, J., Davis, L.C., Galione, A., and Wessel, G. (2007) Flipping the switch: how a sperm activates the egg at fertilization. Dev. Dyn. **236**, 2027-2038.
2. Clapper, D.L., Walseth, T. F., Dargiem P. J, and Lee, H. C. (1987) Pyridine nucleotide metabolites stimulate calcium release from sea urchin egg microsomes desensitized to inositol trisphosphate. J. Biol. Chem. **262**, 9561-9568
3. Lee, H.C., and R. Aarhus (1995) A derivative of NADP mobilizes calcium stores insensitive to inositol trisphosphate and cyclic ADP-ribose. J. Biol. Chem. **270**, 2152-2157

4. Churchill, G. C., Okada, Y., Thomas, J. M., Genazzani, A. A., Patel, S., and Galione, A. (2002) NAADP mobilizes Ca^{2+} from reserve granules, lysosome-related organelles, in sea urchin eggs. Cell **111**, 703-708
5. Morgan, A. J., and Galione, A. (2007) Fertilization and nicotinic acid adenine dinucleotide phosphate induce pH changes in acidic Ca^{2+} stores in sea urchin eggs. J. Biol. Chem. **282**, 37730-37737
6. Morgan, A.J., and Galione, A. (2007) NAADP induces pH changes in the lumen of acidic Ca^{2+} stores. Biochem. J. **402**, 301-310
7. Yamasaki, M., Thomas, J. M., Churchill, G. C., Garnham, C., Lewis, A. M., Cancela, J. M., Patel, S., and Galione, A. (2005) Role of NAADP and cADPR in the induction and maintenance of agonist-evoked Ca^{2+} spiking in mouse pancreatic acinar cells. Curr. Biol. **15**, 874-878
8. Mitchell, K .J., Lai, F. A., and Rutter, G. A. (2003) Ryanodine receptor type I and nicotinic acid adenine dinucleotide phosphate receptors mediate Ca^{2+} release from insulin-containing vesicles in living pancreatic beta-cells (MIN6). J. Biol. Chem. **278**, 11057-11064
9. Zhang, F., Zhang, G., Zhang, A. Y., Koeberl, M. J., Wallander, E., and Li, P. L. (2006) Production of NAADP and its role in Ca^{2+} mobilization associated with lysosomes in coronary arterial myocytes. Am. J. Physiol. Heart Circ. Physiol. **291**, H274-H282
10. Brailoiu, E., Hoard, J. L., Filipeanu, C. M., Brailoiu, G. C., Dun, S L., Patel, S., and Dun, N. J. (2005) Nicotinic acid adenine dinucleotide phosphate potentiates neurite outgrowth. J. Biol. Chem. **280**, 5646-56450
11. Mándi, M., Tóth, B., Timár, G., and Bak, J. (2006) Ca^{2+} release triggered by NAADP in hepatocyte microsomes. Biochem. J., **395**, 233-238
12. Steen, M., Kirchberger, T., and Guse, A. H. (2007) NAADP mobilizes calcium from the endoplasmic reticular Ca^{2+} store in T-lymphocytes. J. Biol. Chem. **282**, 18864-18871
13. Zhang, F. and Li, P. L. (2007) Reconstitution and characterization of a nicotinic acid adenine dinucleotide phosphate (NAADP)-sensitive Ca^{2+} release channel from liver lysosomes of rats. J. Biol. Chem. **282**, 25259-25269
14. Cancela, J.M., Churchill, G. C., and Galione, A. (1999) Coordination of agonist-induced Ca^{2+}-signalling patterns by NAADP in pancreatic acinar cells. Nature **398**, 74-76
15. Churchill, G. C. and Galione, A. (2001) NAADP induces Ca^{2+} oscillations via a two-pool mechanism by priming IP_3- and cADPR-sensitive Ca^{2+} stores. EMBO J. **20**, 2666-2671
16. Calcraft, P. J., Ruas, M, Pan, Z., Cheng, X., Arredouani, A., Hao, X., Tang, J., Rietdorf, K., Teboul, L., Chuang, K. T., Lin, P., Xiao, R., Wang, C., Zhu, Y., Lin, Y., Wyatt, C. N. Parrington, J., Ma, J., Evans, A. M., Galione, A., and Zhu, M. X. (2009) NAADP mobilizes calcium from acidic organelles through two-pore channels. Nature **459**, 596-600
17. Brailoiu, E., Churamani, D., Cai, X., Schrlau, M. G., Brailoiu, G. C., Gao, X., Hooper, R., Boulware, M. J., Dun, N. J., Marchant, J. S., and Patel, S. (2009) Essential requirement for two-pore channel 1 in NAADP-mediated calcium signaling. J. Cell Biol. **186**, 201-209
18. Zong, X., Schieder, M., Cuny, H., Fenske, S., Gruner, C., Rötzer, K., Griesbeck, O., Harz, H., Biel, M., and Wahl-Schott, C. (2009) The two-pore channel TPCN2 mediates NAADP-dependent Ca^{2+}-release from lysosomal stores. Pflugers Arch. **458**, 891-899

19. Brailoiu, E., Hooper, R., Cai, X., Brialoiu, G. C., Keebler, M. V., Dun, N. J., Marchant, J. S., and Patel, S. (2010) J. Biol. Chem. **285,** 2897-2901.
20. Terasaki, M., and Jaffe, L. A. (2004) Labeling of cell membranes and compartments for live cell fluorescence microscopy. Methods Cell. Biol. **74**, 469-489
21. Lee, H. C. and Epel, D. (1983) Changes in intracellular acidic compartments in sea urchin eggs after activation. Dev. Biol. **98,** 446-454
22. Sardet, C. (1983) The ultrastructure of the sea urchin egg cortex isolated before and after fertilization. Dev. Biol. **105**, 196-210
23. Mallya, S. K., Partin, J. S., Valdizan, M. C., and Lennarz, W. J. (1992) Proteolysis of the major yolk glycoproteins is regulated by acidification of the yolk platelets in sea urchin embryos. J. Cell Biol. **117**, 1211-1221
24. Lee, H.C., and Aarhus, R. (2000) Functional visualization of the separate but interacting calcium stores sensitive to NAADP and cyclic ADP-ribose. J. Cell Sci. **113,** 4413-4420
25. Jadot, M., Colmant, C., Wattiaux-De Coninck, S, Wattiaux, R. (1984) Intralysosomal hydrolysis of glycyl-L-phenylalanine 2-naphthylamide. Biochem. J. **219**, 965-970
26. Docampo, R., de Souza, W., Miranda, K., Rohloff, P., and Moreno, S. N. J. (2005) Acidocalcisomes - conserved from bacteria to man. Nat. Rev. Microbiol. **3**, 251-261
27. Ruiz, F. A., Marchesini, N., Seufferheld, M., Govindjee, and Docampo, R. (2001) The polyphosphate bodies of *Chlamydomonas reinhardtii* possess a proton-pumping pyrophosphatase and are similar to acidocalcisomes. J. Biol. Chem. 2001. **276**, 46196-46203
28. Marchesini, N., Ruiz, F. A., Vieira, M., and Docampo, R. (2002) Acidocalcisomes are functionally linked to the contractile vacuole of *Dictyostelium discoideum*. J. Biol. Chem. **277**, 8146-8153
29. Seufferheld, M., Vieira, M., Ruiz, F. A., Rodrigues, C. O., Moreno, S. N. J., and Docampo, R. (2003) Identification of organelles in bacteria similar to acidocalcisomes of unicellular eukaryotes. J. Biol. Chem. **278**, 29971-29978
30. Seufferheld, M., Lea, C. R., Vieira, M., Oldfield, E., and Docampo, R. (2004) The H^+-pyrophosphatase of *Rhodospirillum rubrum* is predominantly located in polyphosphate-rich acidocalcisomes. J. Biol. Chem. **279**, 51193-51202
31. Ruiz, F. A., Lea, C. R., Oldfield, E., and Docampo, R. (2004) Human platelet dense granules contain polyphosphate and are similar to acidocalcisomes of bacteria and unicellular eukaryotes. J. Biol. Chem. **279**, 44250-44257
32. Motta L. S., Ramos I. B., Gomes F. M., de Souza W., Champagne D. E., Santiago M. F., Docampo R., Miranda K. and Machado, E. A. (2009) Proton-pyrophosphatase and polyphosphate in acidocalcisome-like vesicles from oocytes and eggs of *Periplaneta americana*. *Insect Biochem. Molec. Biol.* **39**, 198–206.
33. Ramos, I.B., Miranda, K., Ulrich, P, Ingram, P, LeFurgey, A., Machado, E.A., de Souza, W., and Docampo, R. (2010) Calcium- and polyphosphate-containing acidocalcisomes in chicken egg yolk. Biol. Cell **102**, in press.
34. Ruiz, F. A., Rodrigues, C. O., and Docampo, R. (2001) Rapid changes in polyphosphate content within acidocalcisomes in response to cell growth, differentiation, and environmental stress in *Trypanosoma cruzi.* J. Biol. Chem. 2001. **276**, 26114-26121
35. Ault-Riche, D., Fraley, C D., Tzeng, C M., and Kornberg, A. (1998) Novel assay reveals multiple pathways regulating stress-induced accumulations of inorganic polyphosphate in *Escherichia coli.* J. Bacteriol. **180**, 1841-1847

36. Lanzetta, P. A., Alvarez, L. J., Reinach, P. S., and Candia, O. A. (1979) An improved assay for nanomole amounts of inorganic phosphate. Anal. Biochem. **100**, 95-97
37. Saito, K., Ohtomo, R., Kuga-Uetake, Y., Aono, T., and Saito, M. (2005) Direct labeling of polyphosphate at the ultrastructural level in *Saccharomyces cerevisiae* by using the affinity of the polyphosphate binding domain of *Escherichia coli* exopolyphosphatase. Appl. Environ. Microbiol. **71**, 5692-5701
38. Afzelius, B. A. (1956) The ultrastructure of the cortical granules and their products in the sea urchin egg as studied with the electron microscope. Exp. Cell Res. **10**, 257-285.
39. Lu, H.G., Zhong, L., de Souza, W., Benchimol, M., Moreno, S. N. J., and Docampo, R. (1998) Ca^{2+} content and expression of an acidocalcisomal calcium pump are elevated in intracellular forms of *Trypanosoma cruzi*. Mol. Cell. Biol. **18,** 2309-2323
40. Rodrigues, C. O., Scott, D. A., and Docampo, R. (1999) Characterization of a vacuolar pyrophosphatase in *Trypanosoma brucei* and its localization to acidocalcisomes. Mol. Cell. Biol. **19**, 7712-7723
41. Vercesi, A. and Docampo, R. (1996) Sodium-proton exchange stimulates Ca^{2+} release from acidocalcisomes of *Trypanosoma brucei*. Biochem. J. **315**, 265-270
42. Rodrigues, C.O., Scott, D.A. and Docampo, R. (1999) Presence of a vacuolar H^+-pyrophosphatase in promastigotes of *Leishmania donovani* and its localization to a different compartment from the vacuolar H^+-ATPase. Biochem. J. **340**, 759-766
43. Vercesi, A., Rodrigues, C.O., Catisti, R., and Docampo, R. (2000) Presence of a Na^+/H^+ exchanger in acidocalcisomes of *Leishmania donovani* and their alkalinization by anti-leishmanial drugs. FEBS Lett. **473**, 203-206
44. Maeshima, M. (2001) Tonoplast transporters: organization and function. Annu. Rev.Plant Physiol. Plant Mol. Biol. **52**, 469-497.
45. Ratto, A., and Christen, R. (1988) Purification and characterization of arginine kinase from sea-urchin eggs. Eur. J. Biochem. **173**, 667-674
46. Lemercier, G., Espiau, B., Ruiz, F. A., Vieira, M., Luo, S., Baltz, T., Docampo, R., and Bakalara, N. (2004) A pyrophosphatase regulating polyphosphate metabolism in acidocalcisomes is essential for *Trypanosoma brucei* virulence in mice. J. Biol. Chem. **279**, 3420-3425
47. Rodrigues, C.O., Ruiz, F. A, Vieira, M., Hill, J. E., Docampo, R. (2002) An acidocalcisomal exopolyphosphatase from *Leishmania major* with high affinity for short chain polyphosphate. J. Biol. Chem. **277,** 50899-50906.
48. Johnson, J. D., and Epel, D. (1976) Intracellular pH and activation of sea urchin eggs after fertilisation. Nature **262**, 661-664
49. Shen, S. S., and Steinhardt, R. A. (1978) Direct measurement of intracellular pH during metabolic derepression of the sea urchin egg. Nature **272**, 253-254
50. Epel, D. and Carroll Jr., E. J. (1975) Molecular mechanisms for prevention of polyspermy. Res. Reprod. **7**, 2-3
51. Patel, S. and Docampo, R. (2010) Acidic calcium stores open for business: expanding the potential for intracellular Ca^{2+} signaling. Trends Cell Biol. **20**, 277-286.

Table 1 ^{31}P NMR resonance assignments for perchloric acid extracts of sea urchin eggs

Peak	Assignment	Chemical Shift
A	Phosphorylcholine	3.22
B	Inorganic phosphate	2.60
C	Phosphoarginine	-3.71
D	γ-P of NTP*	-5.66
E	β-P of NDP#	-5.97
F	Inorganic pyrophosphate	-6.29
G	α-P of NDP#	-10.45
H	α-P of NTP*	-10.94
I, J	NAD(H)	-11.39, -12.17
K	NDP-glucose	-12.84
L	Central P of long chain polyphosphate	-20.28
M	β-P of NTP*	-21.21

*NTP, nucleoside triphosphate, #NDP, nucleoside diphosphate

Figure Legends:

Figure 1 Transmission electron microscopy of *Arbacia punctulata* eggs

The preparation was fixed and processed for standard electron microscopy. Cortical granules (cg, *thin arrow*), yolk platelets (YP) and 'clear granules' containing residual electron dense material (*thick arrow*), smaller clear vesicles (*white arrowheads*) and mitochondria (*black arrowheads*) are indicated. Bars in (**A**): 3 µm; (**B**): 1 µm; (**C-E**): 0.5 µm.

Figure 2 Electron microscopy and X-ray microanalysis of whole intact eggs and homogenates

(**A**, and **B**) Electron energy-filtered transmission electron microscopy of an unfixed and unstained egg (**A**) or an egg homogenate (**B**) from *Arbacia punctulata*. Dense granules are identified by black arrows. (**C**), Typical X-ray microanalysis spectrum of dense granules found in egg homogenates (black arrow in (**B**)). (**D**) Typical X-ray microanalysis spectrum of a less electron dense vesicle (probably a yolk platelet) (white arrow in (**B**)) found in egg homogenates. Bars in (**A**), and (**B**): 3 µm.

Figure 3 Detection of PP_i and poly P in sea urchin eggs

(**A**), PP_i, short- (SC) and long-chain (LC) poly P were assayed as described under "Materials and Methods" and levels are expressed as mM poly P (in terms of P_i residues). Data are from 4 experiments, and show means ± S.E.M. Different letters indicate significant differences (one way ANOVA, $p<0.05$). (**B**), Agarose gel electrophoresis of poly P stained with toluidine blue. *Lane 1*: poly P extract; *lane 2*, poly P extract after rPPX1 treatment. P75, P45, and P24 are poly P standards of 75+, 45, and 25 phosphate units. (**C**), 242.8-MHz (^{1}H decoupled) ^{31}P NMR spectra of a perchloric acid extract of sea urchins eggs. See assignments in Table 1. (**D**), differential interferential microscopy of the sea urchin egg shown in (**E**). (**E**), Localization of poly P using the recombinant poly P binding domain of *E. coli* exopolyphosphatase (PPBD) linked with an Xpress epitope tag. Images were deconvolved for 15 cycles using Softwarx deconvolution software. Other conditions are under "Materials and Methods". Bars in (**D**), and (**E**): 15 µm.

Figure 4 Fluorescence microscopy and acridine orange release from dense granule fractions

Dense granule fractions were incubated with 3 µM acridine orange (AO, (**A**, and **C**)) or 10 µg/ml DAPI (**B**, and **D**) as described under "Material and Methods". Note the accumulation of acridine orange ((**A**, and **C**), *orange*) and DAPI ((**B**, and **C**), *yellow*) in vesicles distributed in groups (**A**, and **B**) or isolated (**C**, and **D**). Bars in (**A-D**): 5 µm. (**E**), the dense fraction was diluted in GluIM buffer in the presence of 6 µM AO with and without 10 µM valinomycin (Val) and changes in fluorescence monitored in a fluorometer. Bafilomycin A_1 (Baf, 1 µM) and nigericin (NIG, 1 µM) were added where indicated. *Gray trace* (AO) is the control in the absence of valinomycin. *Light*

grey trace (Control) is the control in the absence of additions. Tracings are representative of 5 experiments. The graph summarizes the changes in fluorescence (ΔF) in (**E**), and is shown as the means ± S.D of 5 determinations expressed as a percentage of the maximal nigericin response. (**F**, and **G**), Dense granule fraction was preincubated with 3 μM acridine orange and 10 μM valinomycin until it equilibrated. (**F**), 100 mM NaCl (*black trace*) or 100 mM KCl (*dark gray trace*) and 5 μM nigericin were added where indicated. (**G**), 10 μM (*black trace*) or 50 μM (*dark gray trace*) $CaCl_2$ and 5 μM nigericin were added where indicated. Control tracings without NaCl or KCl (**F**) or without $CaCl_2$ (**G**) are shown in *light gray*. Tracings in (**F**) and (**G**) are representative of at least 3 experiments The graphs summarize the changes in fluorescence (ΔF) in (**F**) and (**G**), and are shown as the means ± S.D of 3 determinations expressed as a percentage of the maximal nigericin response. Asterisks indicate significant differences (t-test, $P < 0.05$). Ordinates are scaled as RFU (relative fluorescence units) for (**E-G**).

Figure 5 Effects of nigericin on calcium release, acidity, and poly P content of dense granule fractions

(**A**), Dense granule fraction was incubated in GluIM in the presence of Fluo-3, and nigericin (5 μM) was added at the time indicated. (**B**), Dense granule fraction was preincubated with 3 μM acridine orange until it equilibrated, and nigericin (5 μM) was added at the time indicated. (**C**), Short- (SC) and long-chain (LC) poly P levels were measured at different times after addition of 10 μM nigericin. Tracings in (**A**), and (**B**), are representative of at least 4 experiments. Ordinates are scaled as RFU (relative fluorescence units). Controls without nigericin addition (**A**, and **B**) are shown. Graph in (**C**) shows mean ± S.E.M. of 3 experiments. Asterisks in (**C**) indicate significant differences (one-way ANOVA, $P < 0.05$).

Figure 6 Poly P and PP_i hydrolysis in dense granule fractions

Dense granule fractions (DF) were homogenized in GluIM buffer and tested for PPX and PPase activities as described under "Materials and Methods". (**A**), Levels of poly P_3 and poly P_{75+} after different times of incubation of with dense granule fraction. (**B**), Levels of PP_i after different times of incubation with dense granule fraction. Controls (Ctrl) are the substrates incubated in buffer, with no fraction added. Graphs show mean of relative activities ± SEM of 4 experiments. Asterisks indicate significant differences (one-way ANOVA, $P < 0.05$).

Figure 7 Effect of Ca^{2+} releasing agents on poly P content of dense granule fractions

Total homogenates (**A**, and **D**) and dense granule fractions (**B**, and **E**) (310 μg protein in each case) were tested for calcium release triggered by IP_3 and NAADP. Preparations were incubated in GluIM buffer in the presence of 3 μM Fluo-3 as described under "Materials and Methods". IP_3 (300 nM), NAADP (200 nM), and nigericin (5 μM) were added where indicated. Tracings are representative of at least 4 experiments. Controls without additions are shown in *gray*. Ordinates are scaled as RFU (relative fluorescence units). (**C**), and (**F**), the graphs summarize the changes in fluorescence (ΔF) in (**A**) and (**B**), and (**D**) and (**E**), respectively, and are shown as the means ±

S.D. of 3 experiments expressed as a percentage of the maximal nigericin response. Asterisks indicate significant differences (t-test, $P < 0.05$). (**G**), Short-chain poly P levels were measured at different times after addition of increasing NAADP concentrations. Graph shows mean ± S.E.M. of 3 experiments. (**H**), Dense granule fractions (*trace 1*) and total homogenate (*trace 2*) were incubated in GluIM in the presence of 3 µM Fluo-3. GPN (100 µM) and nigericin (5 µM) were added at the times indicated. Control with no additions is shown in *trace 3*. Ordinates are scaled as RFU (relative fluorescence units). (**I**), Graph summarizes the changes in fluorescence (ΔF) in (**H**), and is shown as the means ± S.D of 4 determinations expressed as a percentage of the maximal nigericin response.

Figure 1

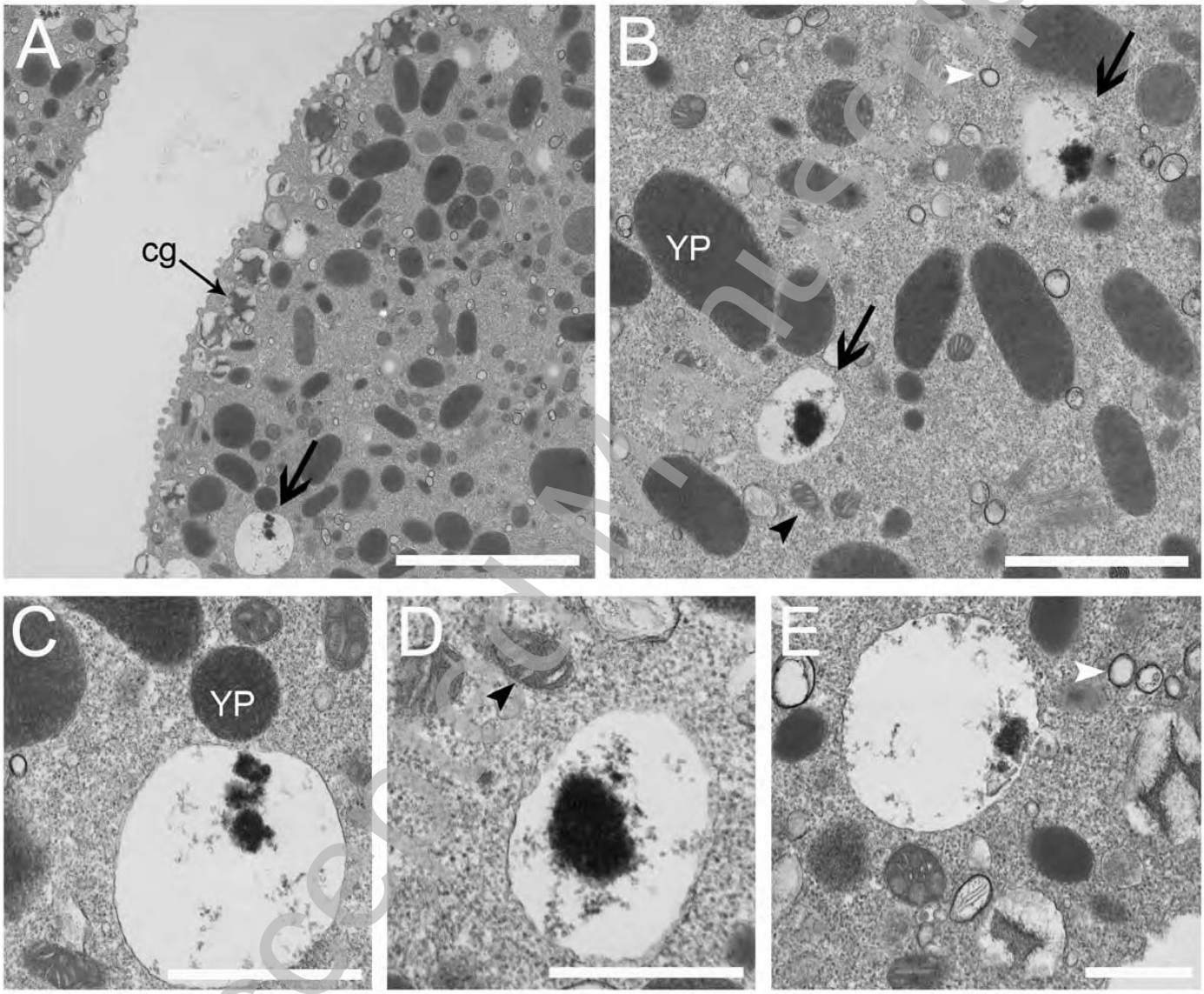

Figure 2

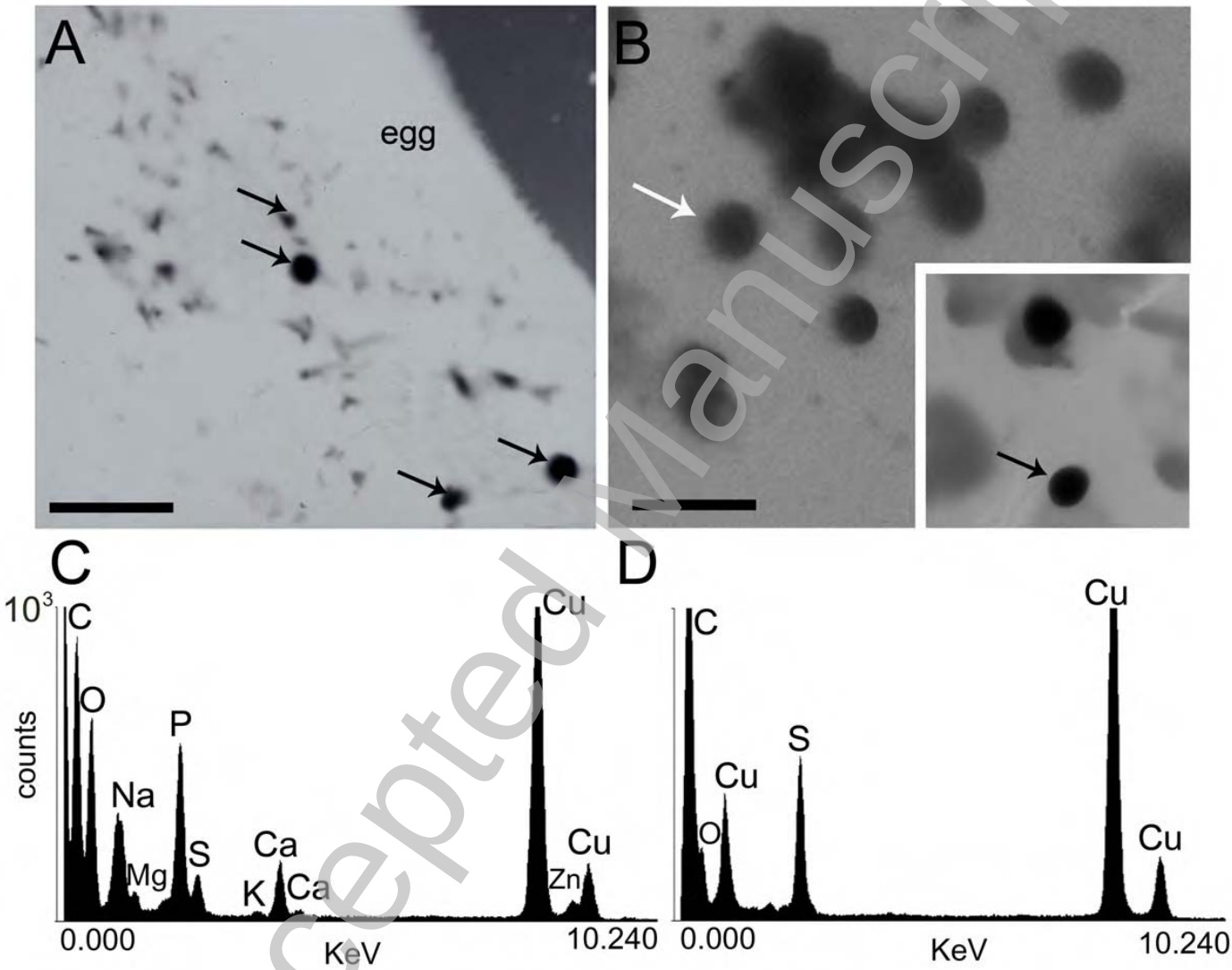

Figure 3

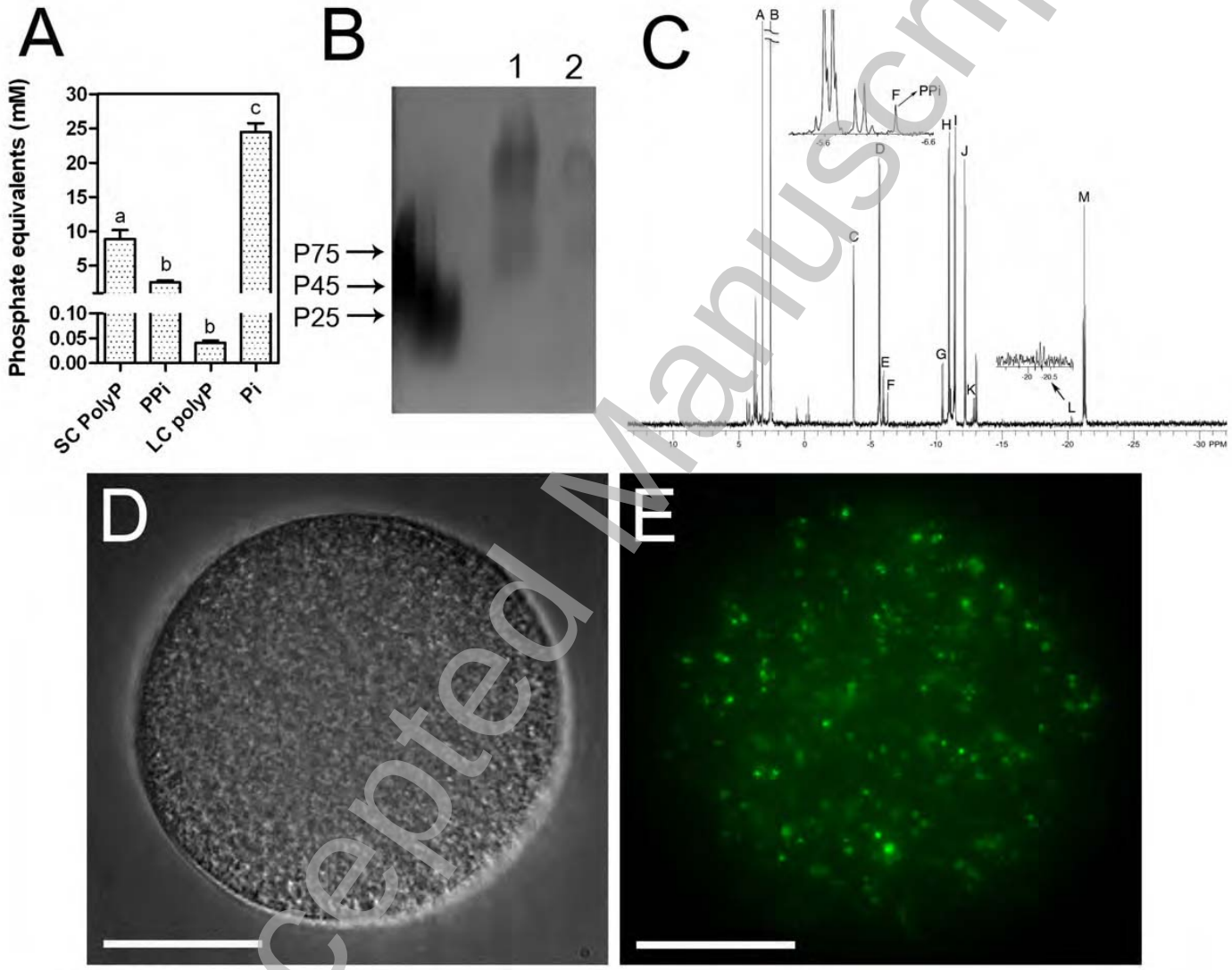

Figure 4

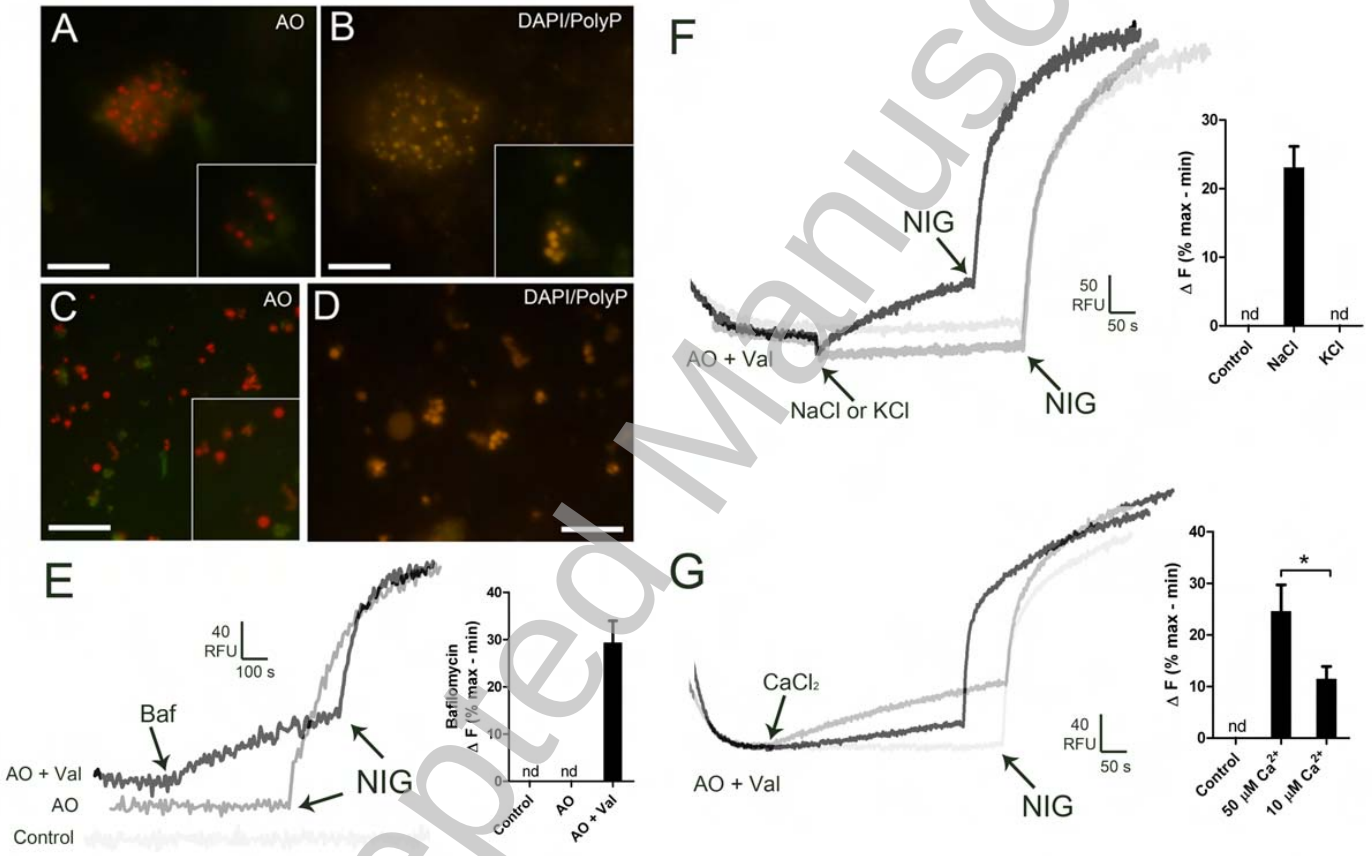

Figure 5

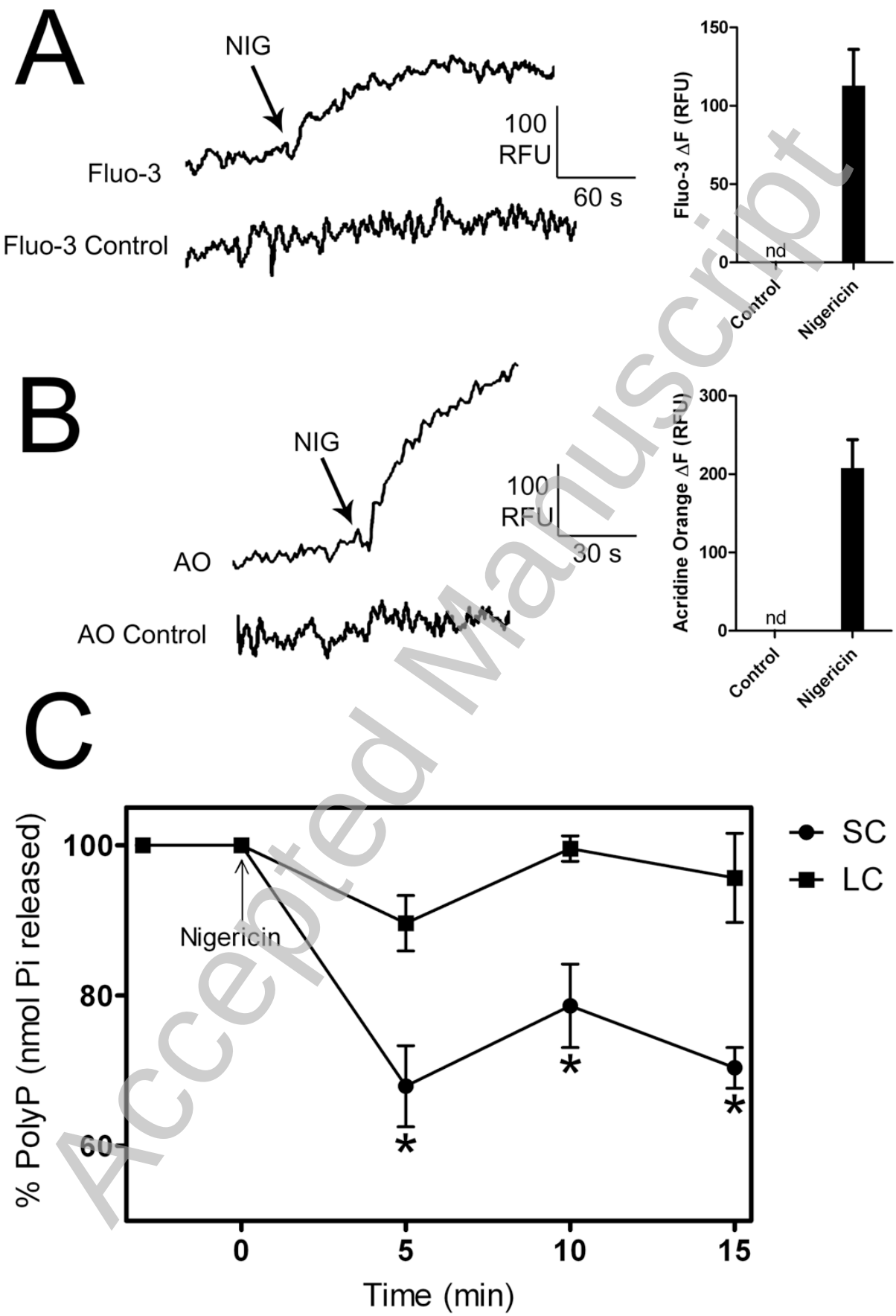

Figure 6

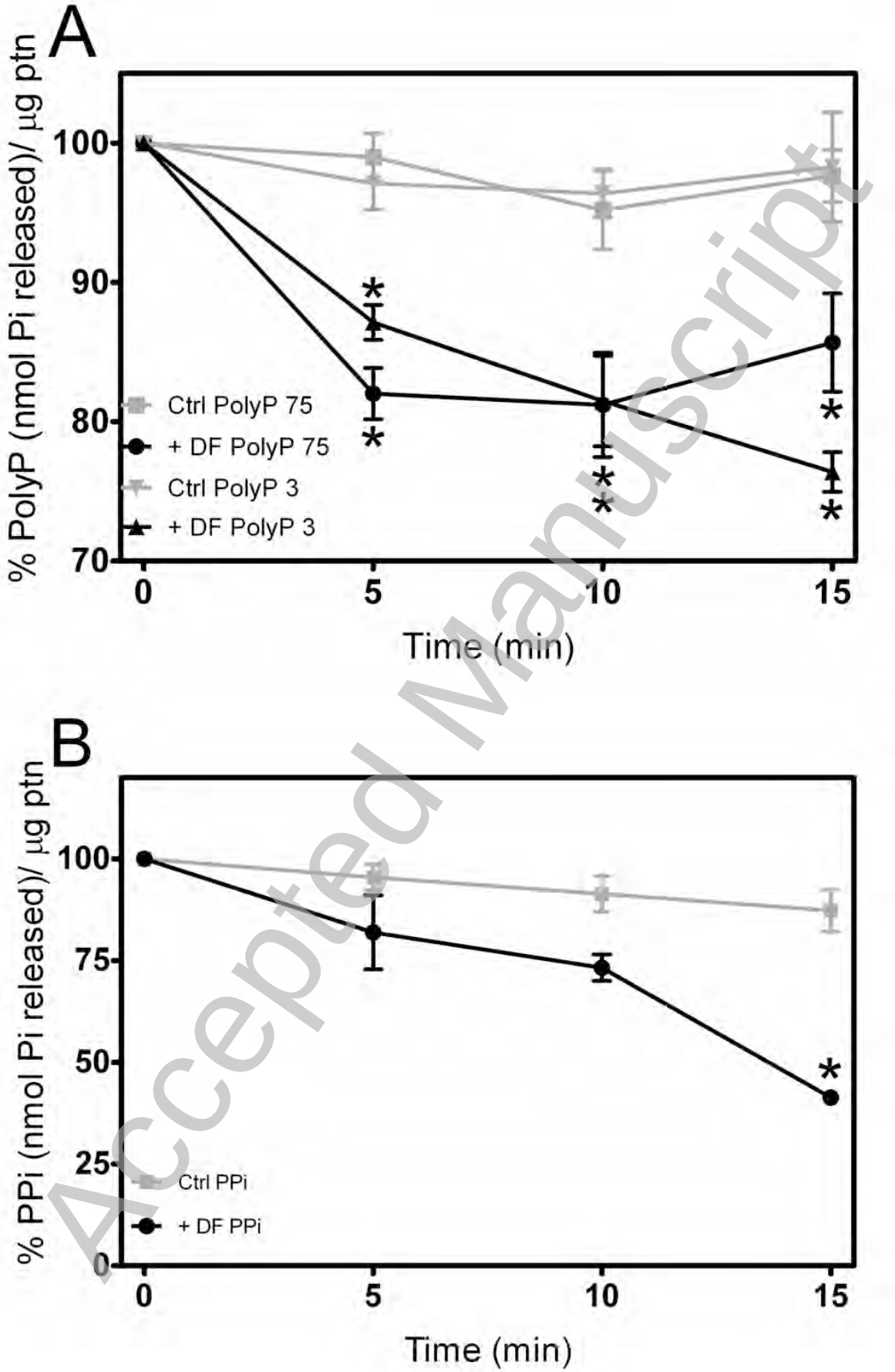

Figure 7